

ANALYSIS AND DESIGN OF TAPERED MEANDER LINE ANTENNAS FOR MOBILE COMMUNICATIONS

Chun-Wen Paul Huang, Atef Z. Elsherbeni, and Charles E. Smith

Electrical Engineering Department, The University of Mississippi
University, MS 38677

Abstract - Small printed antennas are becoming one of the most popular designs in personal wireless communications systems. In this paper, the characterization and design of a novel printed tapered meander line antenna are presented using the finite difference time domain technique. Experimental verifications are applied to ensure the effectiveness of the numerical model, and excellent agreement is found between numerical analysis and prototype measurements. A new design of this antenna features an operating frequency of 2.55 GHz with a 230 MHz bandwidth, which supports future generations of mobile communication systems.

I. Introduction

With the advancements of modern integrated circuit technologies, personal communication systems (PCS) feature light weight, small size, high frequency operation, and high transmission efficiency. Mobile antenna design is one of the major tasks in PCS designs, which requires easy integration with the interior circuitry. One of the most widely used wireless communications systems is the global system for mobile (GSM) communications, which operates at 890-915 MHz for uplink and 935-960 MHz for downlink [12]. The new generation of personal communication systems, such as digital communication systems (DCS) 1800 [12], operates at 1.710-1.785 GHz for uplink and 1.805-1.880 GHz for downlink. Another widely adopted telecommunication system for PCS is the code division multiple access (CDMA) system, which operates at 1.8 to 2.0 GHz. Furthermore, recent designs of indoor cordless phones and modems for wireless local area networks (WLAN), operating at 2.4 GHz of the industrial, scientific, and medical (ISM) band applications, are also available in the market. Therefore, antennas for current and future generation of personal communication systems are designed to operate at a single or dual frequencies in the range from 0.9 GHz to 2.5 GHz. New types of printed meander line antennas have been recently investigated by several authors [1-7]. Detailed studies and empirical formulae of the effects of trace width, segment lengths, and ground plane size of meander line antennas can be found in [8

and 9].

In this paper, studies of the characteristics of a novel tapered meander line antenna [7], using the finite difference time domain (FDTD) [10] techniques with Berenger's perfectly matched layers (PML) [11] absorbing boundaries are presented. The presented designs of the antenna shown in Figure 1, feature small dimensions ($32 \times 25 \times 3.17 \text{ mm}^3$), and approximately 50Ω input impedance with a dual printed sleeve tuner. The antenna is designed to operate at a single frequency within the 0.9-3.0 GHz range on a comparably small ground plane ($59 \times 25.4 \text{ mm}^2$). The validation of the numerical analysis used in this investigation is made by computing the return loss of the tapered antenna and comparing it with measurements. Very good agreement is found using the developed FDTD code. Analysis and design based on this numerical model are thus performed. A wideband design is achieved by using a dual sleeve tuner [2, 6]. The antenna operating bandwidth is centered at 2.5 GHz with 230 MHz of bandwidth. This optimal design can be used for future generation of wireless phones or other current wireless applications operating around this frequency.

II. Design Approach

The antennas considered in this study are shown in Figure 1. In Figure 1(a), a tapered meander line trace is printed on a 25-mm wide dielectric slab sitting on a $59 \times 25.4 \text{ mm}^2$ perfectly conducting ground plane and 1 mm trace width. The parameters e_1 and e_2 represent the lengths of the vertical and horizontal printed traces, respectively. The vertical segment length $e_1 = 2 \text{ mm}$, and the horizontal segment length e_2 starts from 4 mm and ends at 15 mm (5 turns) or 17 mm (7 turns) with a 1 mm increment for each horizontal segment. The corresponding vertical length L_{ax} of the antennas are 25 and 29 mm for 5 turns and 7 turns of tapered meander line traces, respectively. The distance between the edge of the dielectric slab and the edge of the ending segment of the meander line is set equal to e_1 . The reason for modeling the meander line antenna on a small ground plane ($59 \times 25.4 \text{ mm}^2$) is to simulate its performance when this antenna is placed on top of a PCS handset or in other wireless appliances with a

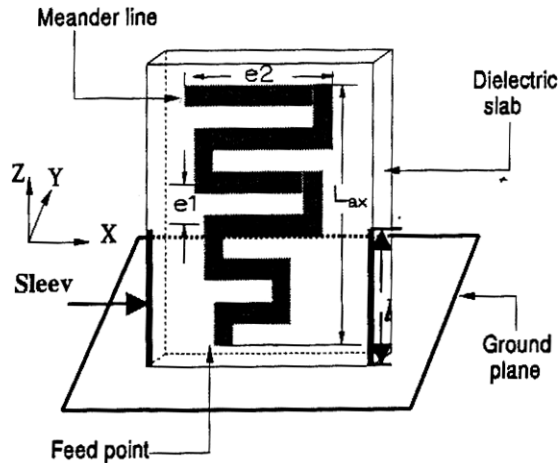


Figure 1(a) An ascendant tapered meander line monopole with dual sleeves on a small ground plane.

small effective ground plane. The main objective of this research is to design a meander line antenna with 50Ω input impedance at an operating frequency within 0.9 to 3.0 GHz. The frequency range under study is extended from 0.9-3.0 GHz to 0.001-10.0 GHz for clearer observations of the resonance behavior of the antenna.

A. FDTD Analysis

The finite difference time domain (FDTD) technique is applied to model the antenna inside a 3-dimensional air chamber terminated with the artificial boundaries of Berenger's perfectly matched layers (PML) [11]. The PML is adopted to reduce the numerical reflection from the truncated boundaries of the finite problem space, which resembles an anechoic chamber for antenna measurements. Eight layers of PML are used in our numerical simulations. An array of voltage sources with a Gaussian waveform is placed between the ground plane and the edge of the first vertical segment of the trace line for excitation. In the numerical simulations, the maximum amplitude of the waveform was set to 1 Volt and the internal resistance of the source was 50Ω . The width of the Gaussian waveform pulse is selected to provide reliable results up to 18 GHz. The simulations are performed for 16,364 time steps with the time increment satisfying the Courant condition. The voltage is sampled between the antenna feed and ground plane, while the current is calculated by applying Ampere's law around the antenna feed, expressed as follows.

$$V(t) = - \int \vec{E}(i, j, k, t) \cdot d\vec{l} \cong - \sum \vec{E}(i, j, k, t) \cdot d\vec{l} \quad (1.a)$$

$$I(t) = - \oint \vec{H}(i, j, k, t) \cdot d\vec{l} \cong - \sum \vec{H}(i, j, k, t) \cdot d\vec{l} \quad (1.b)$$

After the transient voltages and currents are sampled,

their frequency domain representation are calculated using discrete Fourier transform. Hence, the input impedance is obtained by applying

$$Z(f) = \frac{V(f)}{I(f)} \quad (2)$$

The corresponding reflection coefficient of the antenna can be calculated as

$$\Gamma(f) = \frac{Z(f) - R_c}{Z(f) + R_c} \quad (3)$$

R_c is the characteristic impedance of a transmission line, and is always chosen as 50Ω in most RF and wireless communications systems. The return loss of the antenna is calculated using $20 \log |\Gamma(f)|$. The radiation intensity and directive gain of an antenna are defined by equations (4) and (5), respectively.

$$U(\theta, \phi) \cong \frac{|E_\theta(\theta, \phi)|^2 + |E_\phi(\theta, \phi)|^2}{2\eta_0} \quad (4)$$

$$D(\theta, \phi) = 4\pi \frac{U(\theta, \phi)}{\int_0^{2\pi} \int_0^\pi U(\theta, \phi) \sin \theta d\theta d\phi} \quad (5)$$

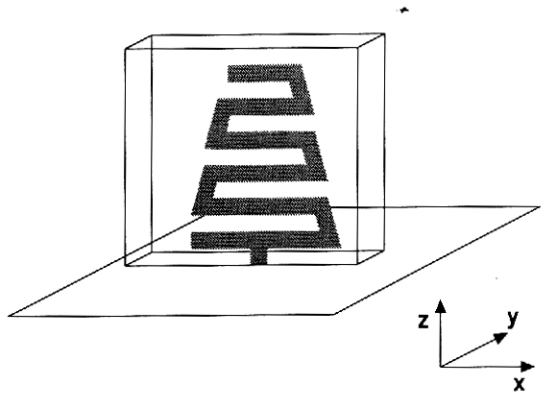
After the characteristics of the tapered meander monopole are analyzed, dual printed sleeves are employed in the design to enlarge the bandwidth and tune the input impedance toward 50Ω . Another tuning method using dual floating printed sleeves is studied, which can be also used to model the behavior of the dual sleeves that are not well grounded.

B. Realization

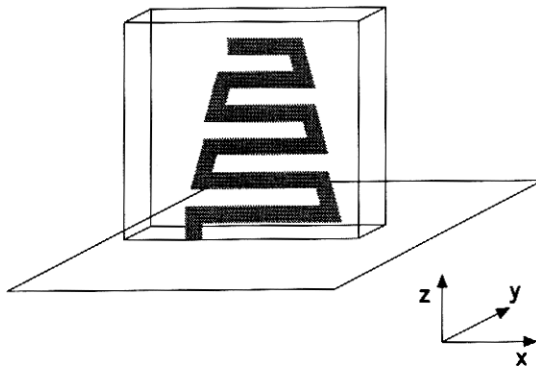
In order to verify the designs obtained from the numerical simulations, tapered meander line antennas with and without dual-sleeve tuners (as shown in Fig. 2) are built and measured. The thickness of the PCB used in building the prototypes of these antennas is one half of that used in the simulations for the optimal design. However, the experimental data based on these prototypes are compared with the simulation results of the same antenna configuration. To prevent bending of this thin dielectric substrate, the width is increased 2 mm more on each side than the width specified in the previous section. The performance of this antenna is measured on a $1.5 \times 2\text{-m}^2$ ground plane to avoid the influence of the scattered fields from surrounding

objects. This ground plane is effective to simulate a semi-infinite ground plane in the frequency range of interest. The test is done using HP 8510C network analyzer, by measuring the return loss over a frequency

the network analyzer reference to the apparent antenna reference plane is obtained. Therefore, the actual electrical delay can be determined by using one half of the time difference between the analyzer reference plane and the total reflection spike, which is 212.5 picosecond for this antenna model. The one half factor is required because the analyzer presents time domain



1(b)



1(c)

Figure 1 Descendant tapered meander line antenna fed (b) centrally and (c) laterally.

range up to 10 GHz. As shown in Fig. 2, there is a 43-mm coaxial cable connected to the fixture of the antenna that serves as an antenna feed. This coaxial cable is excluded in measurement results by applying port extension to compensate for the electrical length of the cable to establish a reference plane at the antenna feed, as determined by time domain reflectometry (TDR).

After calibration, the analyzer is switched to time domain mode, and the antenna characterizations are measured in the time domain. To locate the starting plane of the antenna trace, the antenna is shorted to the ground at the feed point, which results in total reflection with 180 degrees out of phase. Therefore, by locating the reflection with magnitude of 1 and by measuring the time difference between this reflection spike and analyzer's reference plane, the information to translate

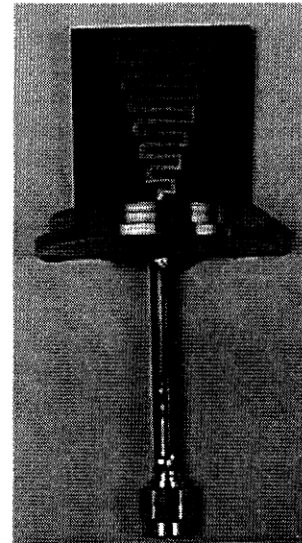


Figure 2 (a) The prototype of a tapered meander line monopole with $e_1 = 2$ mm, e_2 ranges from 3 mm to 17 mm, and a dielectric substrate width of 29 mm.

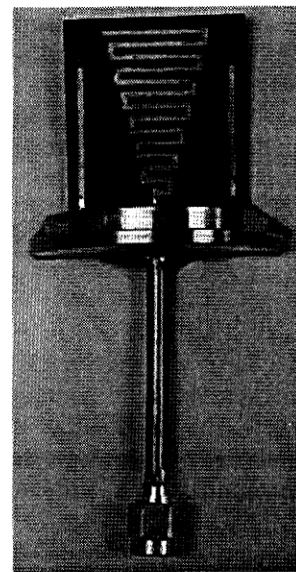


Figure 2(b) The prototype of a dual-sleeve tapered meander line monopole with $e_1 = 2$ mm, e_2 ranges from 3 mm to 17 mm, and a dielectric substrate width of 29 mm.

reflectometry (TDR) data for twice the traveling time between source and load to detect this total reflection. The computed impedance for the taper meander line antenna placed on a semi-infinite ground plane can be obtained by computing half of the meander line dipole configuration impedance, which is analyzed using a cell size of 0.5 mm with 2 cells for modeling the source.

III. Results

The study begins with different ways of tapered meander line layouts. In addition to the tapered line in Figure 1(a), the other tapered meander line layouts, descendant tapered meander line antennas, are shown in Figure 1(b) and (c), which are fed centrally and laterally, respectively. The return losses of these three different types of 5-turn tapered meander line antennas are computed and plotted in Figure 3. From Figure 3, the ascendant type of taper meander monopole has a more desirable wideband characteristic and a better return loss as the frequency increases. Although the side-fed descendant meander line has a very wideband mode, the frequency is too high for PCS applications. Therefore, ascendant tapered meander line antennas are analyzed in this paper and simply referred to tapered meander line antennas.

The first parameter of tapered meander line antennas under study is the effect of the vertical height L_{ax} (or number of turns) on the operating modes. Antennas with 5 and 7 turns of tapered meander traces are analyzed and results are plotted in Figure 4(a). From Figure 4(a), the first and third resonance of the 5-turn tapered meander line antenna occur at 1.9 GHz and 3.98, respectively, which are too high for PCS dual band application. In addition, the resonant impedance is also too small. However, the 7-turn tapered meander line antenna has the first and the third resonance at 1.2 GHz and 2.7 GHz, respectively, which may be tuned as a 50- Ω input impedance antenna for current wireless applications. Therefore, more turns of tapered meander line traces will reduce the operating frequency of the fundamental mode. As observed in Figure 4(a), the operating modes have not only wider bandwidth but also better return loss values as the frequency increases. This 7-turn tapered meander line antenna is also compared with two other types of trace configurations with the same trace length, a printed monopole and equal e_2 (10-mm for the first 4 turns and 11-mm for the last 3 turns) meander line antenna. The reason to adopt the same trace length (161-mm) for all three antennas is to study the resonant characteristics caused by different ways of trace bending. As shown in Figure 4(b), the non-tapered meander line does not have the wideband characteristics like the tapered meander line. In addition, the printed monopole has a repetitive resonant

pattern, but all the operation modes are narrow-band.

To simplify the tuning design, the dual-sleeve method [2, 6] is adopted to improve the input impedance. Because the tapered line is not a uniform segment ratio trace, the optimal sleeve length l is not necessarily $\frac{1}{2}$ of

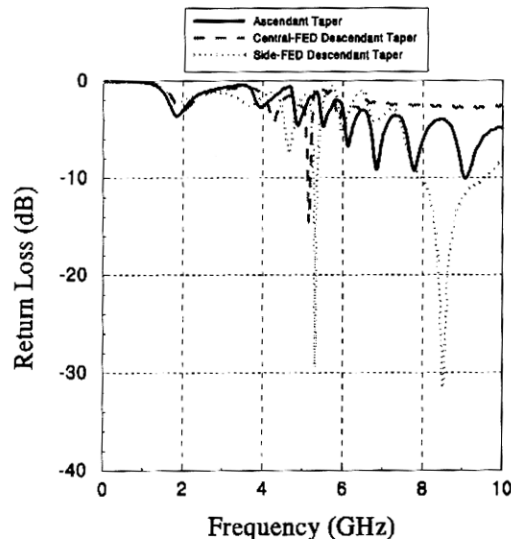


Figure 3 The return losses of ascendant and descendant tapered meander line monopoles.

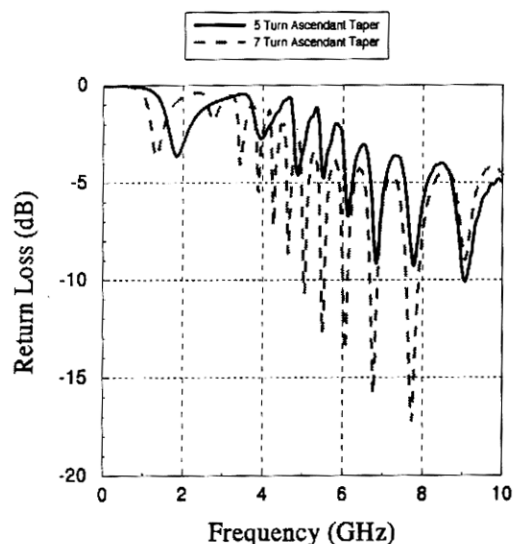


Figure 4(a) The return losses of 5-turn and 7-turn ascendant tapered meander line monopole

L_{ax} , as suggested in [2]. Choosing a spacing of 1mm away from the longest horizontal segment, the effects of different sleeve length is observed in Figure 5(a). From Figure 5(a), the optimal sleeve length for the

lower frequency end is found when the sleeve is 24 mm, 83 % of L_{ax} . Since the optimal sleeve length is determined for the current antenna configuration, the following analysis is made to determine the best location for dual-sleeves. From Figure 5(b), the optimal return loss is found when the spacing between the longest segment and a sleeve is 3 mm (i.e., at the edge

of the substrate. For this case the antenna operates at 2.55 GHz with 230 MHz bandwidth, which is appropriate for future wideband mobile phones and current wireless ISM applications in the vicinity of this frequency. The input impedance at the operating frequency band of this optimal design is shown in Figure 5(c). Small reactance and 50-Ω resistance centered at 2.5 GHz within the operational bandwidth

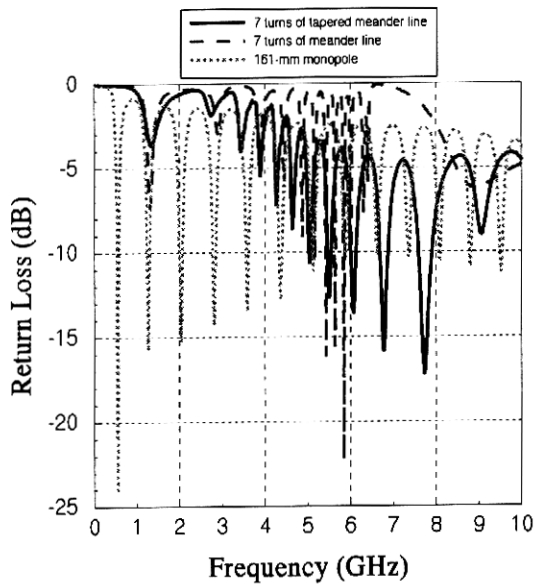


Figure 4(b) The return loss comparisons of a meander line, a tapered meander line, and a monopole antenna with the same trace length (161mm).

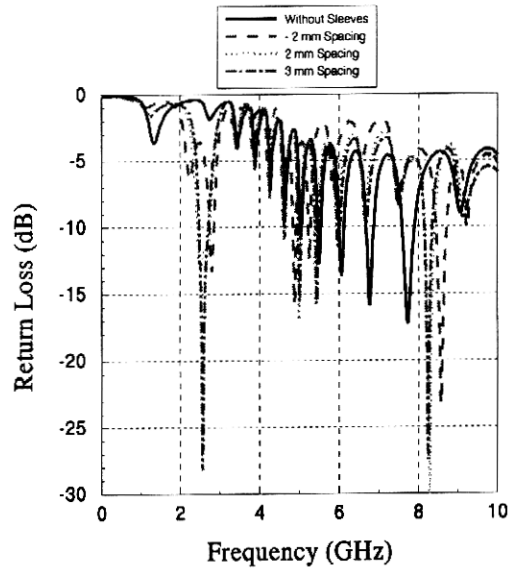


Figure 5(b) Return loss of the tapered meander line monopole versus sleeve spacing.

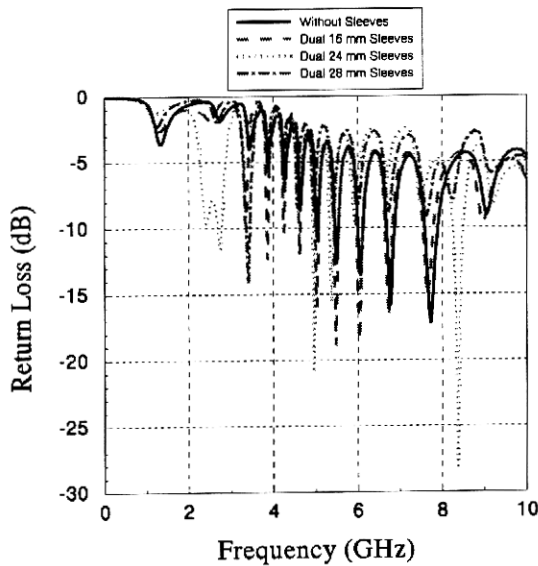


Figure 5(a) Return loss of the tapered meander line monopole versus sleeve length.

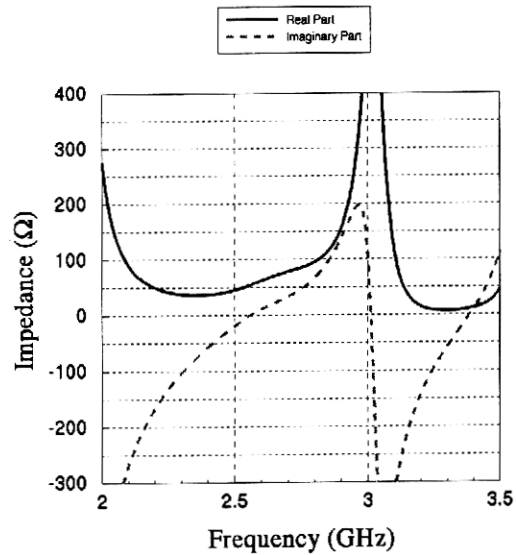
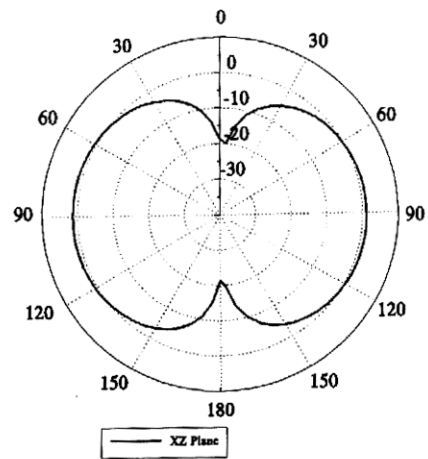
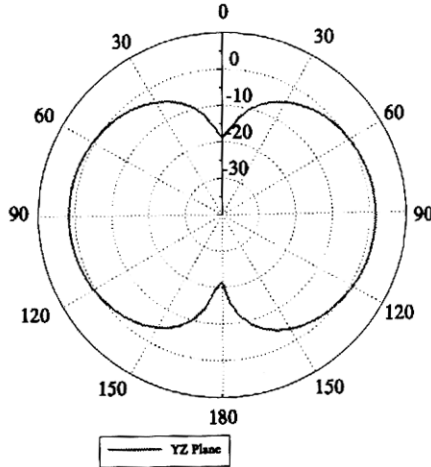


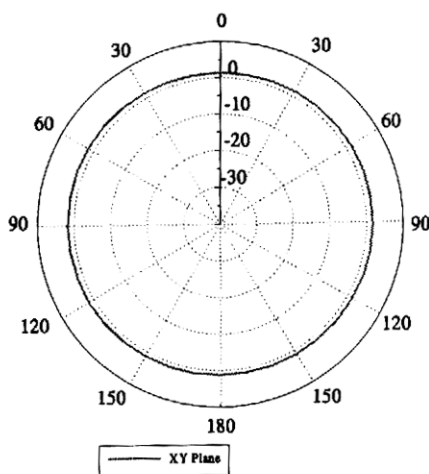
Figure 5(c) Input impedance of the optimal tapered meander line monopole design with 24-mm sleeve and 3-mm away from the longest segment.



(a)



(b)



(c)

Figure 6 The radiation directive gain on (a) xz plane (b) yz plane (c) xy plane at 2.55 GHz.

are observed. The directive gain of this antenna is also computed and patterns in three different planes are shown in Figure 6. From Figure 6, this design has an omni-directional radiation pattern in the xy plane, which is very similar to that of a monopole antenna. From the results in Figures 5(b) and 6, this tapered meander line with dual 24-mm sleeves may be an optimal design for current wireless application.

To analyze the case when the sleeve tuners are not connected to the ground, another study is conducted for dual floating printed lines, as shown in Figure 7(a). The lines are simulated by printed traces at the center of the tapered meander line trace. From Figure 7(b), the effects of floating traces are found to be trivial at frequencies below 5 GHz, but detectable above 5 GHz. From this study, the results indicate that the tuning effectiveness for this application is greatly reduced when the dual sleeves are not well grounded.

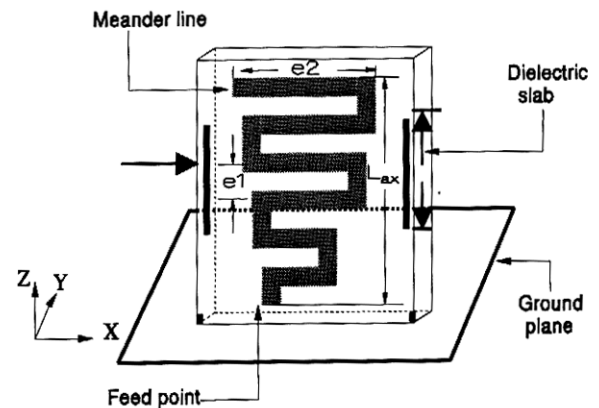


Figure 7(a) Tapered meander line monopole with dual floating lines.

The designs of a tapered meander line antenna with and without dual 24-mm sleeves, as shown in Figure 2, are fabricated and measured. As shown in Figures 8 and 9, agreements are observed up to 10 GHz between the numerical and experimental results. The slight frequency shift in magnitude and phase differences at higher frequencies are mainly accounted by the different feeds used in the numerical and experimental methods and the conductor and dielectric losses at higher frequencies which are not considered in the FDTD simulation. From comparisons of results in Figures 8 and 9, the effectiveness of the numerical model and analyses are reassured.

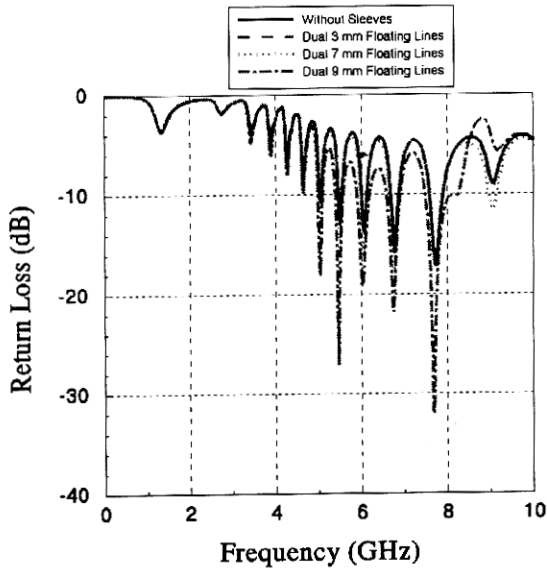


Figure 7(b) Return loss of the tapered meander line monopole versus floating line length.

IV. Conclusions

The reliability of the numerical analyses in this study is demonstrated by comparing FDTD simulations with test results of the prototype antennas. A detailed investigation for optimizing the operating frequency and input impedance of a tapered meander line monopole antenna for wireless communication has been presented. The presented tapered meander line monopoles can be tuned for a broad bandwidth of 230 MHz, operation at 2.55 GHz, and for a 50 Ω input impedance using printed tuning sleeves, which is appropriate for support of current and future generations of wideband wireless communication systems. Optimal results for lower frequency applications, between 1 and 2 GHz, may be achieved by increasing the meander line trace segments or by employing other tuning methods. Future studies will be focused on finding simple tuning methods to tune the lower frequency modes and the optimization of the radiation pattern parameters of the current design.

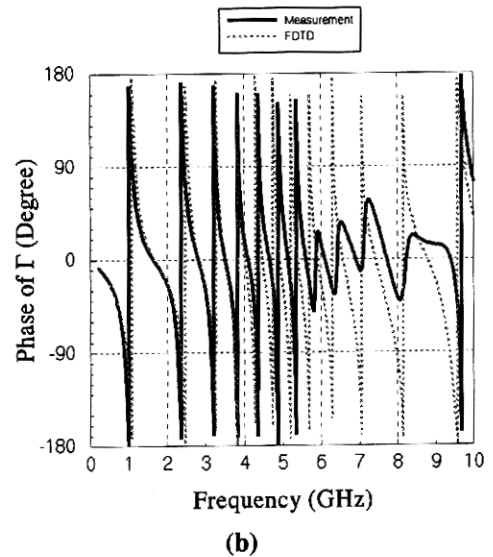
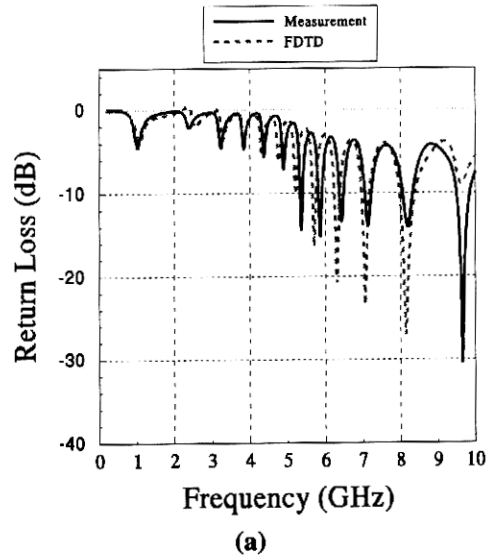


Figure 8 Comparison of the computed and measured (a) return loss (b) phase of the reflection coefficient of the prototyped tapered meander line monopole.

V. Acknowledgement

The authors would like to express their appreciation to Dr. Wen-Liang Wu for his helpful discussions and to Mr. Joon Shin for providing MATLAB programs to visualize the FDTD modelings. In addition, the authors also would like to thank Mr. Po-Leng Chin, Mr. Maqsud Alam, and Mr. Martye Hickman for their efforts on the fabrication of the antenna prototypes.

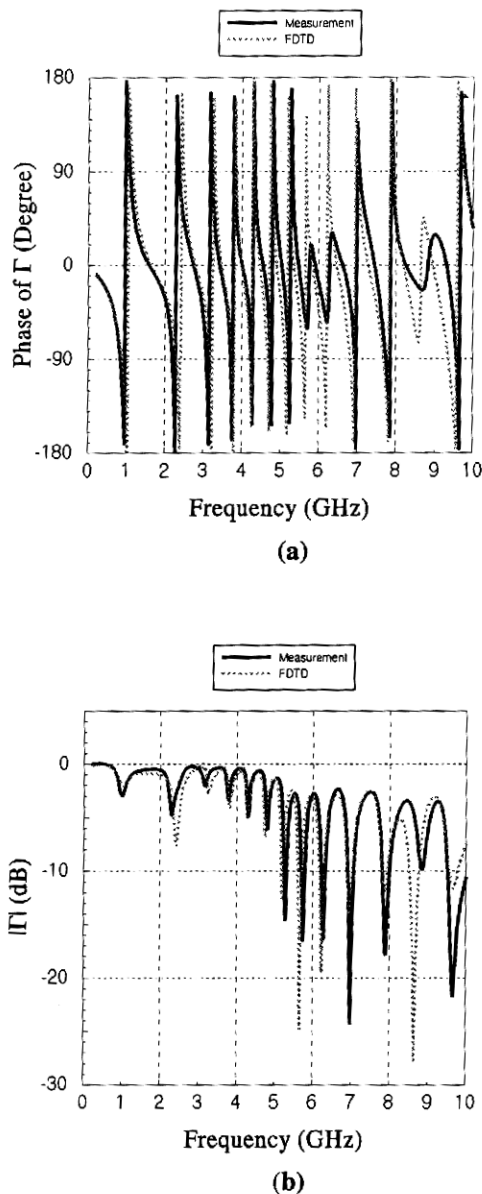


Figure 9 Comparison of measured and FDTD simulation of (a) return loss (b) phase of the reflection coefficient of the dual-sleeve tapered meander line monopole.

REFERENCES

- [1] K. Noguchi, M. Mizusawa, T. Yamaguchi, and Y. Okumura, "Numerical analysis of the radiation characteristics of the meander line antennas consisting of two strips," *IEEE AP-S Digest*, pp. 1598-1601, 1996.
- [2] M. Ali, S. S. Stuchly, and K. Caputa, "A wide-band dual meander-sleeve antenna," *Journal of Electromagnetic Waves and Applications*, vol. 10, no. 9, pp. 1223-1236, 1996.
- [3] A. Z. Elsherbeni, J. Chen, C. E. Smith, and Y. Rahmatt-Sami, "FDTD analysis of meander line antennas for personal communication applications," *Progress in Electromagnetics Research Symposium (PIERS)*, Cambridge, MA, 1997.
- [4] M. Ali, S. S. Stuchly, and M. Okoniewski, "Characterization of planar printed meander line antennas using the finite difference time domain technique," *IEEE AP-S Dig.*, pp. 1546-1549, 1997.
- [5] H. Y. Wang and M. J. Lancaster, "Aperture-coupled thin-film superconducting meander line antennas," *IEEE Trans. Antennas Propagat.*, vol. 47, no.5, pp. 829-836, May 1999.
- [6] C. P. Huang, A. Z. Elsherbeni, J. J. Chen, and C. E. Smith, "FDTD characterization of meander line antennas for RF and wireless communications," *Progress in Electromagnetics Research Symposium (PIERS)*, vol. 24, pp. 185-200, 1999.
- [7] C. P. Huang, A. Z. Elsherbeni, and C. E. Smith, "FDTD analysis of tapered meander line antennas for RF and wireless communications," the 16th Annual Review of Progress in Applied Computational Electromagnetics (ACES), March, 2000.
- [8] C. P. Huang, "Analysis and design of printed antennas for wireless communications using finite difference time domain technique," Ph.D. dissertation, Dept. Electrical Engineering, Univ. of Mississippi, Dec. 1999.
- [9] A. Z. Elsherbeni, C. P. Huang, and C. E. Smith, "Finite difference time domain analysis of printed meander line antennas for personal wireless communications," Dept. Electrical Engineering, Univ. of Mississippi, technical report No. TR 001, Jan. 2000.
- [10] K. S. Yee, "Numerical solution of initial boundary value problems involving Maxwell's equations in isotropic media," *IEEE Trans. Antennas Propagat.*, vol. 14, pp. 202-307, 1966.
- [11] J. P. Berenger, "A perfectly matched layer for the absorption of electromagnetic waves," *J. Computat. Phys.*, Oct. 1994.
- [12] K. D. Katsibas, C. A. Balanis, P. A. Tirkas, and C. R. Birtcher, "Folded loop antenna for mobile handheld units," *IEEE Trans. Antennas Propagat.*, vol. 46, no. 2, pp. 260-266, Feb. 1998.